

1 **Uncertainty analysis of eddy covariance CO₂ flux**
2 **measurements for different EC tower distances using an**
3 **extended two-tower approach**

4 **H. Post¹, H.J. Hendricks Franssen¹, A.Graf¹, M. Schmidt¹, H. Vereecken¹**

5 [1] {Agrosphere (IBG-3), Forschungszentrum Jülich GmbH, 52425 Jülich, Germany}

6

7 **Abstract**

8 The use of eddy covariance CO₂ flux measurements in data assimilation and other
9 applications requires an estimate of the random uncertainty. In previous studies, the
10 (classical) two-tower approach has yielded robust uncertainty estimates, but care must be
11 taken to meet the often competing requirements of statistical independence (non-overlapping
12 footprints) and ecosystem homogeneity when choosing an appropriate tower distance. The
13 role of the tower distance was investigated with help of a roving station separated between 8
14 m and 34 km from a permanent EC grassland station. Random uncertainty was estimated for
15 five separation distances with the classical two-tower approach and an extended approach
16 which removed systematic differences of CO₂ fluxes measured at two EC towers. This
17 analysis was made for a dataset where (i) only similar weather conditions at the two sites
18 were included, and (ii) an unfiltered one. The extended approach, applied to weather-filtered
19 data for separation distances of 95 m and 173 m gave uncertainty estimates in best
20 correspondence with an independent reference method. The introduced correction for
21 systematic flux differences considerably reduced the overestimation of the two-tower based
22 uncertainty of net CO₂ flux measurements and decreased the sensitivity of results to tower
23 distance. We therefore conclude that corrections for systematic flux differences (e.g. caused
24 by different environmental conditions at both EC towers) can help to apply the two-tower
25 approach to more site pairs with less ideal conditions.

26 **Keywords:** Eddy covariance, measurement uncertainty, random error, NEE, footprint,
27 systematic flux differences

28 **1 Introduction**

29 The net ecosystem exchange of CO₂ between the land surface and the atmosphere (*NEE*) can
30 be determined with the eddy covariance (EC) method. Eddy covariance CO₂ flux
31 measurements are commonly used to analyze the interactions between terrestrial ecosystems
32 and the atmosphere which is crucial for the understanding of climate-ecosystem feedbacks. In
33 this regard reliable EC data with appropriate uncertainty estimates are crucial for many
34 application fields, such as the evaluation and improvement of land surface models (e.g.
35 Braswell et al., 2005; Hill et al., 2012; Kuppel et al., 2012).

36 When using the term ‘uncertainty’, we here focus on the random error following the
37 definition in Dragoni et al. (2007). It differs from the systematic error in that it is
38 unpredictable and impossible to correct (but can be quantified). Uncertainty doesn’t
39 accumulate linearly but “averages out” and can be characterized by probability distribution
40 functions (Richardson et al., 2012). Systematic errors are considered to remain constant for a
41 longer time period (> several hours). Ideally they can be corrected, but in case of EC
42 measurements this is still limited by either our understanding of various error sources or
43 insufficient background data. Systematic errors arise not only from instrumental calibration
44 and data processing deficits, but also from unmet underlying assumptions about the
45 meteorological conditions (Richardson et al., 2012). A main assumption is that turbulence is
46 always well developed in the lowest atmospheric boundary layer and responsible for the mass
47 transport while horizontal divergence of flow and advection are assumed to be negligible
48 (Baldocchi, 2001). Moreover, the EC method is based on the mass conservation principle,
49 which requires the assumption of steady state conditions of the meteorological variables
50 (Baldocchi, 2003). In case of CO₂ fluxes, night-time respiration is often underestimated due
51 to low wind velocities conditions and a temperature inversion which hinders the upward

52 carbon dioxide transport (Baldocchi, 2001). Hence, night-time data are commonly rejected
53 for further analysis (Barr et al., 2006).

54 After a possible correction of the EC flux data for systematic errors a random error will
55 remain which can arise from different sources such as (a) the assumption of a constant
56 footprint area within a measurement interval and the negligence of flux footprint
57 heterogeneity (e.g. due to temporal variability of wind direction, wind speed and atmospheric
58 stability which cause temporal variations of the footprint area); (b) turbulence sampling errors
59 which are related to the fact that turbulence is a highly stochastic process and especially the
60 sampling or not sampling of larger eddies is associated with considerable random fluctuations
61 of fluxes, even if they are already averaged over a 30-minutes period; and (c) instrumentation
62 deficits that can e.g. cause random errors in the measured variables (such as the CO₂ mixing
63 ratio and the vertical wind velocity) used to calculate the net CO₂ flux (Aubinet et al., 2011,
64 p. 179; Flanagan and Johnson, 2005).

65 Within the past decade, several approaches have been proposed to quantify the uncertainty of
66 eddy covariance CO₂ flux measurements. With the “two-tower” or “paired tower” approach
67 simultaneous flux measurements of two EC towers are analyzed (Hollinger et al., 2004;
68 Hollinger and Richardson, 2005). For the uncertainty quantification with the two-tower
69 approach, it is necessary that environmental conditions for both towers are nearly identical
70 (Hollinger et al., 2004; Hollinger and Richardson, 2005). However, most eddy covariance
71 sites do not have a nearby second EC tower to provide nearly identical environmental
72 conditions. Therefore, Richardson et al. (2006) introduced the “one-tower” or “24-h
73 differencing” method which is based on the two-tower approach. The main difference is that
74 the uncertainty estimate is based on differences between fluxes measured on subsequent days
75 if environmental conditions were similar on both days. Because most often environmental

76 conditions are not the same on two subsequent days (Liu et al., 2006), the applicability of this
77 method suffers from a lack of data and the random error is overestimated (Dragoni et al.,
78 2007). The model residual approach (Dragoni et al., 2007; Hollinger and Richardson, 2005;
79 Richardson et al., 2008) calculates CO₂ fluxes with a simple model and compares calculated
80 values with measured values. The model residual is attributed to the random measurement
81 error. The method is based on the assumption that the model error is negligible, which is
82 however a very questionable assumption. Alternatively, if the high-frequency raw-data of an
83 EC tower are available, uncertainty can be estimated directly from their statistical properties
84 (Billesbach, 2011). Finkelstein and Sims (2001) introduced an operational quantification of
85 the instrumental noise and the stochastic error by calculating the auto- and cross-covariances
86 of the measured fluxes. This method was implemented into a standard EC data processing
87 scheme by Mauder et al. (2013). The advantage is that a second tower or the utilization of
88 additional tools such as a simple model to estimate the EC measurement uncertainty is no
89 longer required. However, many data users do not have access to the raw-data but to
90 processed EC data only. Moreover, a large amount of solid metadata about the setup of the
91 EC measurement devices is required (but often not provided at second hand) to obtain
92 reliable raw-data based uncertainty estimates adequately. Therefore a two-tower based
93 approach has still a large group of users. In particular with regard to pairs of nearby towers
94 from local clusters which play an increasing role in the monitoring strategies of e.g. ICOS
95 and NEON, and have already been employed in case studies (e.g. Ammann et al., 2007).
96 Important advantages of the two-tower approach are (1) its simplicity and user friendliness,
97 (2) its usability for relatively short non gap-filled time series of several months, and (3) the
98 independence of a model.

99 The classical two-tower approach (Hollinger et al., 2004; Hollinger and Richardson, 2005;
100 Richardson et al., 2006) is based on the assumption that environmental conditions for both

101 EC towers are identical and flux footprints should not overlap to guarantee statistical
102 independence. Hollinger and Richardson (2005) use threshold values for three variables
103 (photosynthetically active photon flux density PPF, temperature & wind speed) to
104 determine whether environmental conditions are equivalent. Independent of this definition,
105 our understanding of “environmental conditions” includes both weather conditions and land
106 surface properties such as soil properties (texture, density, moisture, etc.), plant
107 characteristics (types, height, density, rooting depth, etc.), nutrient availability and fauna
108 (microorganisms, etc.), which are irregularly distributed and affect respiration and/or
109 photosynthesis. Strictly speaking, if footprints do not overlap 100%, the assumption of
110 identical environmental conditions is already not fulfilled. When applying a two-tower based
111 approach it is important to assure that systematic differences of the measured fluxes, which
112 are partly caused by within site or among site heterogeneity, are not attributed to the random
113 error estimate of the measured *NEE*. Our assumption that even within a site with apparently
114 one uniformly distributed vegetation type (and for very short EC tower distances) land
115 surface heterogeneity can cause significant spatial and temporal variability in measured *NEE*
116 is e.g. supported by Oren et al. (2006). They found that the spatial variability of ecosystem
117 activity (plants and decomposers) and LAI within a uniform pine plantation contributes to
118 about half of the uncertainty in annual eddy covariance *NEE* measurements while the other
119 half is attributed to micrometeorological and statistical sampling errors. This elucidates the
120 relevance of considering systematic flux differences caused by within site ecosystem
121 heterogeneity when calculating a two-tower based uncertainty estimate.

122 Given the fact that site specific, adequate uncertainty estimates for eddy covariance data are
123 very important but still often neglected due to a lack of resources, we are aiming to advance

124 the two-tower approach so that it can also be applied if environmental conditions at both eddy
125 covariance towers are not very similar.

126 The main objectives of this study were (1) to analyze the effect of the EC tower distance on
127 the two-tower based CO₂ flux measurement uncertainty estimate and (2) to extend the two-
128 tower approach with a simple correction term that removes systematic differences in CO₂
129 fluxes measured at the two sites. This extension follows the idea of the extended two-tower
130 approach for the uncertainty estimation of energy fluxes presented in Kessomkiat et al.
131 (2013). The correction step is important for providing a more reliable random error estimate.
132 In correspondence with these objectives we analyzed the following questions: What is an
133 appropriate EC tower distance to get a reliable two-tower based uncertainty estimate? Can the
134 random error be quantified in reasonable manner with the extended two-tower approach, even
135 though environmental conditions at both EC towers are clearly not identical? The total
136 random error estimated with the raw-data based method (Mauder et al., 2013) was used as a
137 reference to evaluate our extended two-tower approach based results.

138 **2 Test sites and EC Tower setup**

139 The Rollesbroich test site is an extensively used grassland site, located in the Eifel region of
140 western Germany (Fig.1). The mean temperature in Rollesbroich is ~ 7.7°C and the mean
141 precipitation is ~ 1033mm per year (Korres et al., 2010). Predominating soil types at the site
142 are Cambisols with a high clay and silt content (Arbeitsgruppe BK50, 2001). The grass
143 species grown in Rollesbroich are mainly ryegrass, particularly perennial ryegrass (*lolium*
144 *perenne*), and smooth meadow grass (*poa pratensis*) (Korres et al., 2010). A permanent eddy
145 covariance tower (EC1) is installed at the Rollesbroich site since May 2011 at a fixed
146 position. The measurement height of the sonic anemometer (CSAT3, Campbell Scientific,

147 Logan, UT, U.S.A.) and the open-path gas analyzer (Li7500, Li-Cor, Lincoln, NE, U.S.A.) is
148 2.6 m above ground. The canopy height was measured every 1-2 weeks and varied between
149 0.03 m and 0.88 m during the measurement period. A second EC tower, the roving station
150 (EC2), has been installed at four different distances (8 m, 95 m, 173 m and 20.5 km) from
151 EC1 for time periods ranging between 3 and 7.5 months (Tab.1). The EC2 location “Kall-
152 Sistig” 20.5 km north-east of Rollesbroich is another grassland site with similar
153 environmental conditions as Rollesbroich. The vegetation in Kall-Sistig is extensively
154 managed C3 grass, the same as for Rollesbroich. However, the average plant height measured
155 between Aug. 14th and Oct. 30th 2012 was lower (~ 0.15 m) than the respective average for
156 Rollesbroich (~ 0.2 m), which is also true for the plant height measured in May and June
157 2012 (Kall-Sistig: ~ 0.22 m; Rollesbroich: ~ 0.29 m). As in Rollesbroich, clayey-silty
158 Cambisols are most widespread (Arbeitsgruppe BK50, 2001). The mean temperature for the
159 entire measurement interval in Kall-Sistig (Tab.1) measured at the EC station is 11.4 °C and
160 the soil moisture 32% compared to 11.0 °C and 35% in Rollesbroich (same time interval for
161 averaging). Additionally a third EC tower was located in Merzenhausen in ~ 34 km distance
162 to EC1 (Fig.1). Merzenhausen (MH) is an agricultural site, where winter wheat was grown
163 during the measurement period. Both the land use conditions and the average weather
164 conditions differ from those in Rollesbroich and Kall-Sistig. The climate at the lowland site
165 Merzenhausen is comparable to the one in Selhausen at a distance of 13 km from
166 Merzenhausen, where the mean precipitation is ~ 690 mm/a and the yearly mean temperature
167 ~9.8°C (Korres et al., 2010). The soils are mainly Luvisols with some patches of Kolluvisols
168 (Arbeitsgruppe BK50, 2001). The measurement devices of EC2 and EC3 are the same as the
169 EC1 devices and were installed 2.6 m above ground as well. Both, the sonic anemometers
170 and the open-path gas analyzers have been calibrated every 1-3 months thoroughly and
171 consistently. Details on the EC data acquisition are summarized in Sect. 3.1.

172 Rollesbroich is part of the TERENO network (Zacharias et al., 2011). Information and
173 additional data were collected showing that land surface properties are spatially
174 heterogeneous distributed at the Rollesbroich site: (1) Single fields at the Rollesbroich site
175 are managed by different farmers. Information the land owners provided, as well as periodic
176 camera shots and grass height measurements around the EC towers indicated that the timing
177 of fertilization and grass cutting as well as the amount of manure applied varied between the
178 single fields during the measurement period; (2) Soil type distribution as displayed in the
179 German soil map shows heterogeneity (Arbeitsgruppe BK50, 2001); (3) Soil carbon and
180 nitrogen pools [g/kg] as well as bulk density [g/cm³] and content of rock fragments [%]
181 measured from April-May 2011 in three soils horizons at 94 locations across the Rollesbroich
182 site are spatially highly variable (H. Schiedung 2013, personal communication); (4) During
183 the eddy covariance measurement period, soil moisture and soil temperature data were
184 collected in 10 min. resolution at three depths (5 cm, 20 cm and 50 cm) and 84 points by the
185 wireless sensor network (“SoilNet”; Bogaen et al., 2009), calibrated for the Rollesbroich site
186 by Qu et al., (2013). SoilNet data shows that soil moisture is heterogeneously distributed
187 within the Rollesbroich site (Qu et al., 2014).

188 **3 Data and Methods**

189 **3.1. EC data processing**

190 The EC raw data were measured with a frequency of 20 Hz and fluxes were processed for
191 flux intervals of 30 minutes. The complete processing of the data was performed with the
192 TK3.1 software (Bayreuth, Department of Micrometeorology, Germany; Mauder and Foken,
193 2011), using the standardized strategy for EC data calculation and quality assurance
194 presented in detail by Mauder et al., 2013. The strategy includes established EC conversions

195 and corrections such as e.g. correction of spectral loss (Moore, 1986) and correction for
196 density fluctuations (Webb et al., 1980). It includes tests on high frequency data (site specific
197 plausibility limits, statistical spike detection) as well as on processed half hourly fluxes such
198 as stationarity and integral turbulence tests (Foken and Wichura, 1996). The tests on half
199 hourly fluxes are the basis for a standardized quality flagging according to Mauder and Foken
200 (2011) that classifies flux measurements as high (0), moderate (1) or low (2) quality data. For
201 this analysis only flux measurements assigned to 0 or 1 were used, while low quality data
202 were treated as missing values. Besides quality flags TK3.1 also provides footprint estimates
203 (Kormann and Meixner, 2001) and uncertainty estimates that were used for interpreting and
204 analyzing flux data. To avoid introduction of additional uncertainty no gap filling of flux time
205 series was performed.

206 **3.2. Uncertainty estimation based on the two-tower approach**

207 The two-tower approach (Hollinger et al., 2004; Hollinger and Richardson, 2005; Richardson
208 et al., 2006) defines the random error of *NEE* eddy covariance measurements as the standard
209 deviation $\sigma(\delta)$ of the difference between the CO₂ fluxes [$\mu\text{mol m}^{-2}\text{s}^{-1}$] simultaneously
210 measured at two different EC towers (NEE_1, NEE_2):

$$\sigma(\delta) = \frac{\sigma(NEE_1 - NEE_2)}{\sqrt{2}} \quad \text{Eq. 1}$$

211 Based on Eq.1 we calculated the two-tower based uncertainty estimates using the NEE_1 data
212 measured at the permanent EC tower in Rollesbroich (EC1) and the NEE_2 data of a second
213 tower which was either the roving station (EC2) or – in case of the 34 km EC tower distance
214 – another permanent EC tower (EC3, Tab.1).

215 For comparison, the measurement uncertainty $\sigma(\delta)$ was calculated separately for each EC
216 tower distance (Tab.1) and independently for each of the following schemes:

- 217 1. The classical two-tower approach (Hollinger et al., 2004; Hollinger and Richardson,
218 2005; Richardson et al., 2006).
- 219 2. The classical two-tower approach including a filter for similar weather conditions
220 (Sect. 3.4).
- 221 3. The extended two-tower approach with an added correction for systematic flux
222 differences (sfd-correction; Sect. 3.3), without weather-filter.
- 223 4. The extended two-tower approach with sfd-correction and the previously applied
224 weather-filter.

225 The uncertainty estimate of the two-tower approach is obtained by dividing the *NEE* data
226 series into several groups (“bins”) according to the flux magnitude and then using Eq. 1 to
227 calculate the standard deviation $\sigma(\delta)$ for each group (Richardson et al., 2006). Finally, a
228 linear regression function between the flux magnitude and the standard deviation can be
229 derived. The linear correlation of the uncertainty and the flux magnitude can be explained by
230 the fact that the flux magnitude is a main driving factor for the random error and can explain
231 about 63% of the variance in the CO₂ flux error as shown in a case study by Richardson et al.
232 (2006). Accordingly, we calculated the standard deviation $\sigma(\delta)$ [$\mu\text{mol m}^{-2} \text{s}^{-1}$] based on 12
233 groups of the CO₂ flux magnitude; six groups for positive and six groups for negative fluxes.
234 (*NEE* is positive if the amount of CO₂ released to the atmosphere via respiration is higher
235 than the amount of CO₂ assimilated during photosynthesis. In contrast, negative *NEE* values
236 denote a higher CO₂ uptake and a net flux from the atmosphere into the ecosystem.) Fixed
237 class limits for the flux magnitude would have led to a different number of samples in each
238 group. Now class limits were set such that all groups with positive *NEE* values had an equal

239 amount of half hourly data, the same holds for all groups with negative *NEE* values. For each
240 single group the standard deviation $\sigma(\delta)$ was calculated using the single half-hourly flux
241 differences of NEE_1 and NEE_2 . The corresponding mean *NEE* magnitude for each group
242 member was determined by averaging all half-hourly means of NEE_1 and NEE_2 in the
243 respective group. Then, the linear regression equation was derived separately for negative and
244 positive *NEE* values using the 6 calculated standard deviations $\sigma(\delta)$ and the 6 mean *NEE*
245 values. This procedure was carried out for each dataset of the five EC tower distances and
246 again for each of the four uncertainty estimation schemes so that altogether 20x2 linear
247 regression equations were derived. The significance of the correlation between the *NEE*
248 magnitudes and the standard deviations $\sigma(\delta)$ was tested with the *p*- value determined with the
249 Student's t-test based on Pearson's product moment correlation coefficient *r*. Moreover, the
250 95% confidence intervals of the slope and the intercept for each liner regression equation
251 were determined. The linear regression equations were calculated imposing as constraint an
252 intercept ≥ 0 , because a negative standard deviation is not possible. With those linear
253 regression equations, the uncertainty for the individual half-hourly *NEE* measurement values
254 of the permanent EC tower in Rollesbroich (EC1) were estimated using the individual half-
255 hourly NEE_1 values [$\mu\text{mol m}^{-2} \text{s}^{-1}$] as input (x) to calculate the corresponding uncertainty
256 $\sigma(\delta)$ [$\mu\text{mol m}^{-2} \text{s}^{-1}$] (y).

257 The described calculation of the individual *NEE* uncertainty values was done for all half
258 hourly *NEE* data, including those data points that were discarded by the weather filter
259 (Sect.3.4) and/or the sfd-correction (Sect.3.3). Hence, for each of the four two-tower based
260 uncertainty estimation schemes the same amount of individual *NEE* uncertainty values was
261 generated. These mean uncertainty estimates were used to evaluate the effect of the EC tower
262 distance as well as the sfd-correction and the weather-filter on the two-tower based

263 uncertainty estimation. Even though Hollinger et al. (2004) and Richardson and Hollinger
264 (2005) already pointed out that the two-tower approach assumes similar environmental
265 conditions and non-overlapping footprints, we applied the classical approach for all EC tower
266 distances, even if these basic assumptions were not fulfilled, to allow for a comparison of the
267 results before and after the usage of the weather-filter and the sfd-correction (extended two-
268 tower approach).

269 **3.3. Correction for systematic flux differences (sfd-correction)**

270 Different environmental conditions and other factors such as instrumental calibration errors
271 can cause systematic flux differences between two towers. Because these flux differences are
272 not inherent to the actual random error of the measured *NEE* at one EC tower station they
273 lead to an overestimation of the two-tower approach based uncertainty. Therefore, we
274 extended the classical two-tower approach with a simple correction step for systematic flux
275 differences (sfd-correction). The reason why systematic flux differences can statistically be
276 separated quite easily from random differences of the EC flux measurements is their
277 fundamentally different behavior in time: random differences fluctuate highly in time
278 whereas systematic differences tend to be constant over time or vary slowly. The sfd-
279 correction introduced is similar to the second correction step in Kessomkiat et al. (2013,
280 Equation 6 therein), but adapted to the measured *NEE* instead of latent and sensible heat
281 fluxes. An averaging time interval of 12 hours was used to calculate the running mean for the
282 sfd-correction. For each moving average interval, the mean NEE_{12h} of one EC tower
283 (separately for EC1 and EC2) [$\mu\text{mol m}^{-2} \text{s}^{-1}$] and the mean CO_2 flux averaged over both EC
284 towers NEE_{2T_12h} [$\mu\text{mol m}^{-2} \text{s}^{-1}$] were calculated to define the sfd-correction term which was
285 used to calculate the corrected NEE_{corr} [$\mu\text{mol m}^{-2} \text{s}^{-1}$]:

$$NEE_{corr} = \frac{NEE_{2T,12hr}}{NEE_{12h}} \cdot NEE \quad \text{Eq. 2}$$

286 *NEE* is the single half-hourly, processed *NEE* value [$\mu\text{mol m}^{-2} \text{s}^{-1}$] of one EC tower. Only if
 287 both *NEE* data, *NEE*_{-EC1-} for the permanent EC1 tower and *NEE*_{-EC2-} for the second tower,
 288 were available at a particular half hourly time step and if both values were either positive or
 289 negative, the respective data were included to calculate the correction term. The running
 290 averages were only calculated if at least 50% of the data for *NEE*_{-EC1-} and *NEE*_{-EC2} remained
 291 for averaging in that particular window. Due to the frequent occurrence of gaps in the data
 292 series the amount of available *NEE*_{corr} values considerably decreased by applying stricter
 293 criteria like 70% or 90% data availability (Tab. A2). We assume a 12 hour averaging period
 294 to be long enough to exclude most of the random error part but short enough to consider daily
 295 changes of systematic flux differences. For a six hour interval for instance the uncertainty of
 296 the mean *NEE* is usually higher. For larger window sizes (24 or 48 hours) further analysis
 297 was hampered by too many data gaps, i.e. the 50% criterion was hardly ever fulfilled and not
 298 enough averages remained to allow for the two-tower based uncertainty estimation (Tab. A2).
 299 The correction was done separately for positive and negative fluxes, due to the different
 300 sources, properties and magnitudes of the CO₂ flux measurements and different errors for
 301 daytime (negative) and night-time (positive) fluxes (e.g. Goulden et al., 1996; Oren et al.,
 302 2006; Wilson et al., 2002).

303 The final sfd-corrected *NEE1*_{corr} values for EC1 and *NEE2*_{corr} values for EC2 should not be
 304 understood as corrected *NEE* flux data. They were used only to enhance the two-tower based
 305 uncertainty estimation in a way that systematic flux differences which cause an
 306 overestimation of the uncertainty are filtered out. Moreover, systematic flux differences at

307 two EC towers are not to be confused with systematic errors, which are independent of the
308 uncertainty estimation method and optimally corrected before the random error is estimated.

309 **3.4. Filter for weather conditions**

310 For larger distances of two EC towers, such as the 20.5 km and 34 km distance in this study,
311 different weather conditions can cause differences of the measured fluxes in addition to the
312 different land surface properties. Some weather variables (e.g. temperature) are following a
313 clear diurnal and annual course and differences in e.g. temperature at two EC towers are
314 therefore relatively constant. This is expected to cause rather systematic differences in the
315 measured *NEE* which can be captured with the sfd-correction. However, other variables such
316 as wind speed or incoming short wave radiation are spatially and temporally much more
317 variable, for example related to single wind gusts or cloud movement. Differences in the
318 measured fluxes at two EC towers caused by those spatial-temporally highly variable weather
319 variables cannot be captured well with the sfd-correction term due to this “random character”.
320 However, a weather filter can account for this because it compares the differences in weather
321 variables at each single time step. Therefore a filter for similar weather conditions was
322 applied in addition to the sfd-correction following Hill et al. (2012) and Richardson et al.
323 (2006) to only include half hourly *NEE* data, if the weather conditions at the second EC tower
324 are similar to those at the permanent EC1 tower location in Rollesbroich. Following the
325 definition in Richardson et al. (2006), similar weather conditions were defined by a
326 temperature difference $< 3^{\circ}\text{C}$; wind speed difference $< 1\text{ m/s}$ and difference in PPFD < 75
327 $\mu\text{mol m}^{-2}\text{ s}^{-1}$. The weather-filter was applied before the (classical) uncertainty estimation and
328 the sfd-correction. As shown e.g. in Tsubo and Walker (2005), the incoming short wave
329 radiation (or solar irradiance SI) and the photosynthetically active radiation (PAR) are
330 linearly correlated. Accordingly SI and PPFD measured at the EC1 station in Rollesbroich

331 were also linearly correlated. Because direct PPFD measurements were not available for all
 332 measurement periods, we derived a linear regression equation on the basis of all SI and PPFD
 333 data for the permanent EC tower station (EC1). Using this equation, missing PPFD values
 334 were estimated if only SI but no PPFD data were available at a certain time step.

335 **3.5. Footprint analysis**

336 The footprint analysis was applied to quantify the percentage footprint overlap of the two EC-
 337 stations during the measurement periods. This information was not used to filter the data but
 338 to allow for a better understanding of the mean uncertainty estimates for the different
 339 scenarios. Using the analytical model of Kormann and Meixner (2001) implemented in the
 340 TK3.1 software (Mauder and Foken, 2011), a grid of estimated source weights (resolution 2
 341 m, extension 1 km by 1 km) was computed for each half-hour and station position. The
 342 overlap between the footprints of two simultaneously measuring towers was then quantified
 343 as:

$$O_{12}(t) = \sum_{x=1}^N \sum_{y=1}^M \min(f_1(x, y, t), f_2(x, y, t)) \quad \text{Eq. 3}$$

344 The indices 1 and 2 indicate the tower and t the time (in our case, half-hour). N and M are the
 345 number of pixels in east-west and north-south direction, x and y the respective running
 346 indices. The minimum function $\min()$ includes the source weight f computed for the
 347 respective tower, x and y location, and half-hour. O is 1 if both source weight grids are
 348 identical, and 0 in case of no overlap. During stable conditions, the footprint area of a tower
 349 increases and can result in considerable source weight contributions from outside the
 350 modeling domain. Assuming that two footprints which overlap highly in the modeling
 351 domain likely continue to overlap outside the modeling domain, O as defined above might be

352 low-biased in such cases. We therefore additionally considered a normalized version
353 $O/\min(\Sigma\Sigma f_I, \Sigma\Sigma f_I)$ as an upper limit estimate of the overlap. The overlap for the additional
354 sites Kall and Merzenhausen more than 20 km away was assumed zero.

355 **3.6. Comparison measures**

356 To compare and evaluate the two-tower based uncertainty estimates, we calculated random
357 error estimates based on Mauder et al. (2013) as a reference. This reference method is
358 independent of the two-tower based approach, because data of only one EC tower are used to
359 quantify the random error of the measured fluxes and raw data instead of the processed fluxes
360 are used. The raw-data based random error estimates – the instrumental noise σ_{cov}^{noise} and the
361 stochastic error σ_{cov}^{stoch} – were calculated independently. Mauder et al. (2013) determine the
362 instrumental noise based on signal autocorrelation. Following Finkelstein and Sims (2001)
363 the stochastic error is calculated as the statistical variance of the covariance of the flux
364 observations. Generally, σ_{cov}^{noise} was considerably lower than σ_{cov}^{stoch} . The total raw-data based
365 random error σ_{cov} [$\mu\text{mol m}^{-2}\text{s}^{-1}$] was calculated by adding σ_{cov}^{noise} and σ_{cov}^{stoch} “in quadrature”

366 ($\sigma_{cov} = \sqrt{\sigma_{cov}^{stoch^2} + \sigma_{cov}^{noise^2}}$) according to Aubinet et al. (2011, p.176). The mean reference
367 σ_{cov} used for the evaluation of the two-tower based random error estimates was calculated
368 by averaging the single half-hourly σ_{cov} values for the permanent EC1 tower in Rollesbroich.
369 In order to be consistent with the two-tower based calculations, exactly the same half hourly
370 time steps of the EC1 data series used for the two-tower based uncertainty estimation were
371 used to calculate the corresponding mean reference values σ_{cov} . As indicator for the
372 performance of the two-tower based uncertainty estimation schemes applied for the five
373 different EC tower distances, the relative difference $\Delta \sigma_{cov}$ [%] of a two-tower based
374 uncertainty value [$\mu\text{mol m}^{-2}\text{s}^{-1}$] and σ_{cov} [$\mu\text{mol m}^{-2}\text{s}^{-1}$] was calculated:

$$\Delta\sigma_{cov}[\%] = \frac{\sigma(\delta) - \sigma_{cov}}{\sigma_{cov}} * 100 \quad \text{Eq. 4}$$

375 Then, $\Delta\sigma_{cov}$ values were compared for the different EC tower separation distances and two-
 376 tower based uncertainty estimation schemes. The performance of the two-tower based
 377 uncertainty estimation was considered better if $\sigma_{cov}[\%]$ was closer to zero.

378 **4 Results**

379 **4.1. Classical two-tower based random error estimates**

380 Fig.2 and Fig.3 show the linear regressions of the random error $\sigma(\delta)$ (also referred to as
 381 “standard error” or “uncertainty”) as function of the *NEE* magnitude according to the
 382 classical two-tower approach for the different EC tower distances without weather-filter
 383 (Fig.2) and with weather-filter (Fig.3). The dashed linear regression lines denote that the
 384 linear correlation between $\sigma(\delta)$ and *NEE* is weak ($p > 0.1$), which is in particular true for the
 385 positive *NEE* values measured for 173 m and 20.5 km EC tower distances as well as for the
 386 negative *NEE* values for 20.5 km and 34 km distance. The 95% confidence intervals of the
 387 respective slopes and the intercepts are summarized in the Appendix (Tab.A1). Uncertainty
 388 estimation with the classical two-tower approach is critical for those larger distances because
 389 measured flux differences caused by different environmental conditions at both EC towers
 390 can superimpose the random error signal which e.g. originates from instrumental or
 391 turbulence sampling errors. This weakens the correlation of the random error and the flux
 392 magnitude. This is not surprising since Hollinger et al. (2004) and Richardson and Hollinger
 393 (2005) already pointed out that similar environmental conditions are a basic assumption of

394 the two-tower approach. Therefore, statements of how the weather filter affects the mean
395 uncertainty estimate $\sigma(\delta)$ for those large distances need to be treated with caution.

396 The weather-filtering only increased the correlation between the flux magnitude and the
397 random error $\sigma(\delta)$ for positive fluxes for separation distances of 173 m and 20 km whereas in
398 most cases the linear correlation was weakened, mainly due to a decreased number of
399 samples in each averaging group of the *NEE* flux magnitude. Therefore, testing stricter
400 weather-filter criteria (e.g. wind speed < 0.5 m/s, PPFD < 50 $\mu\text{mol m}^{-2} \text{s}^{-1}$, Temp < 2 °C),
401 which caused a decline of samples in each group from e.g. $n > 1000$ to 24 or less, resulted in
402 little meaningful results.

403 As illustrated in Tab.2, the mean *NEE* uncertainty estimate based on the classical two-tower
404 approach increased as a function of EC tower distance. However, without applying the
405 weather-filter, the mean uncertainty $\sigma(\delta)$ was nearly identical for the two largest distances
406 (20.5 km and 34 km), although e.g. the land cover and management in Merzenhausen (EC3
407 tower at 34 km separation) were different from the Rollesbroich site. As a result of the
408 weather-filtering, the mean uncertainty was less overestimated for the distances 173m and
409 20.5 km. However, for the 95 m and 34 km distance, the overestimation of the uncertainty
410 estimate increased by the weather-filtering (Tab.2). This implies that for the classical two-
411 tower approach (without sfd-correction) weather-filtering did not clearly reduce the
412 overestimation of the uncertainty for largest EC tower distances (20.5 km and 34 km) where
413 weather-filtering is expected to be particularly relevant.

414 Comparing the mean uncertainty estimates of the classical two-tower approach with the
415 reference random error estimates σ_{cov} , indicates that both with and without weather filter the
416 uncertainties were overestimated (Tab.2), for all EC tower differences. This could be

417 expected for the large distances, because basic assumptions for the application of the classical
418 two-tower approach are violated for these large distances. But results illustrate that even for
419 short EC tower distances NEE uncertainty estimated with the classical two-tower approach is
420 larger than the raw-data based estimates (Tab.2).

421 **4.2. Extended two-tower approach**

422 The scatter plots in Fig.4 illustrate the effect the sfd-correction (Eq.2) had on the difference
423 of the NEE data simultaneously measured at both EC towers (NEE_{-EC1-} and NEE_{-EC2-}). The
424 sfd-correction reduced the bias and scattering, because systematic differences of the
425 measured fluxes, e.g. induced by different environmental conditions, were removed. As
426 expected, the effect of the sfd-correction was considerably higher for the larger EC tower
427 distances because environmental conditions are also expected to differ more if the distance of
428 two locations is larger. For the 8 m EC tower distance for instance, the effect of the sfd-
429 correction is very minor because footprints are often nearly overlapping. However, for the EC
430 tower distances ≥ 173 m, the bias and scattering of NEE_{-EC1-} and NEE_{-EC2-} was considerably
431 reduced by the sfd-correction.

432 A comparison of Fig.2 and Fig.5 illustrates how the sfd-correction affected the linear
433 regression of the NEE standard error as function of NEE flux magnitude: The sfd-correction
434 considerably enhanced the correlation of NEE_{corr} and the standard error $\sigma(\delta)_{corr}$ for the EC
435 tower distances 20.5 km and 34 km from $R^2 \geq 0.15$ to $R^2 \geq 0.43$.

436 Applying the sfd-correction (without weather-filter) reduced the mean uncertainty value by
437 41.6% to 56.9% for the EC tower distances from 8m to 34 km. The relative differences $\Delta \sigma_{cov}$
438 indicate that the correction for systematic flux differences considerably improved the two-
439 tower based uncertainty estimate for the distances >8 m (Tab.2): The difference $\Delta \sigma_{cov}$ was

440 notably smaller ($< 56.8\%$) for all distances except the 8 m distance compared to $\Delta \sigma_{cov}$
441 determined with the classical two-tower approach ($< 274.7\%$). The most considerable
442 improvement was achieved for the 95 m EC tower distance and the 173 m distance.
443 Additional application of the weather-filter (Fig.6) on the sfd-corrected NEE_{corr} data reduced
444 the mean uncertainty estimate $\sigma(\delta)_{corr}$ by 23.3% and 2.9% for the 20.5 km and the 34 km EC
445 tower distance and reduced $\Delta \sigma_{cov}$ by 57.7% and 7.7%. The effect of the weather-filter on the
446 uncertainty estimates of the shorter EC tower distances was very minor (Tab.2). The
447 uncertainty estimates $\sigma(\delta)_{corr,f}$ determined with the extended two-tower approach agree best
448 with the independent reference values σ_{cov} for the EC tower distances 95m and 173 m,
449 suggesting that those distances were most suitable for the application of the extended two-
450 tower approach.

451 **4.3. Discussion**

452 The results show that the two-tower based uncertainty estimates (both classical and extended
453 two-tower approach) were smallest for the 8 m distance. This can be explained with the
454 results of the footprint analysis: While the average percentage footprint overlap is 13%
455 (normalized 19%) for the 95 m EC tower distance and only 4% (7%) for the 173m EC tower
456 distance, it is 68% (80%) for the 8 m EC tower distance. The stronger overlap of the 8 m
457 distance footprint areas is associated with a more frequent sampling of the same eddies. As a
458 consequence, part of the random error was not captured with the two-tower approach. If EC
459 towers are located very close to each other (< 10 m) and the footprint overlap approaches
460 100%, only instrumental errors and stochasticity related to sampling of small eddies will be
461 captured with the two-tower based uncertainty estimate. Because the EC measurements are
462 statistically not independent if the footprints are overlapping, the classical EC tower method

463 is not expected to give reliable uncertainty estimates for very short EC tower distances
464 (Hollinger et al., 2004; Hollinger and Richardson, 2005). However, without applying the sfd-
465 correction, the mean uncertainty estimate $\sigma(\delta)$ was higher than the raw-data based reference
466 value σ_{cov} which includes both the instrumental noise σ_{cov}^{noise} and the stochastic error σ_{cov}^{stoch} .
467 The raw-data based σ_{cov}^{noise} itself was only $0.04 \mu\text{mol m}^{-2} \text{s}^{-1}$ of $0.64 \mu\text{mol m}^{-2} \text{s}^{-1}$ for the
468 dataset of the 8 m EC tower distance. The mean uncertainty value derived with the extended
469 two-tower approach $\sigma(\delta)_{corr,f}$ for the same dataset was lower than $\sigma(\delta)$ but still considerably
470 higher than σ_{cov}^{noise} , suggesting that even at 8 m EC tower distance instrumentation errors were
471 only a minor part of the two-tower based uncertainty estimate. For the larger separation
472 distances 95 m or 173 m with notably less footprint overlap turbulence sampling errors are
473 almost fully accounted for by a two-tower approach. (It should be noted that forest stations,
474 with a typically larger aerodynamic measurement height and footprint size, will require larger
475 separation distances). However, different land surface properties and management are more
476 likely for the larger separation distances and can cause systematic flux differences that should
477 not be attributed to the random error estimate. As outlined in section 2, land surface
478 properties related to management (e.g. nutrient availability due to fertilization), soil properties
479 (bulk density, skeleton fraction), soil carbon-nitrogen pools, soil moisture and soil
480 temperature are heterogeneously distributed at the Rollesbroich site. The effect of soil
481 moisture, soil temperature and soil properties on CO_2 fluxes (respiration mainly) is well
482 known (e.g. Herbst et al., 2009; Flanagan and Johnson, 2005; Xu et al., 2004; Lloyd and
483 Taylor, 1994; Orchard and Cook, 1983) as well as the role of grassland management (e.g.
484 Allard et al., 2007). Results indicate that an overestimation of the two-tower based
485 uncertainty caused by different land surface properties in the footprint area of both EC towers
486 can be successfully filtered out by the extended approach. It should be noted that a shorter
487 moving average interval of the sfd-correction term (e.g. 6 hours instead of the applied 12

488 hours window; Tab.A2), results in slightly lower uncertainty estimates compared to the
489 reference. This can be explained by a possible “over-correction” of the *NEE* data related to a
490 too short moving average interval for calculating the sfd-correction term. It needs to be
491 emphasized that the estimated mean *NEE* values of the moving average intervals are
492 associated with uncertainty. As mentioned, the moving average interval should be long
493 enough to exclude random differences of the simultaneously measured fluxes but short
494 enough to limit the impact of non-stationary conditions. However, the 12hr running mean
495 *NEE1* and *NEE2* values (NEE_{12}) as well as the respective means of *NEE1* and *NEE2*
496 ($NEE_{2T_{12}}$) used to calculate NEE_{corr} (Eq.2) are uncertain because they still contain the
497 random error part which cannot be corrected or filtered out. This uncertainty in the mean is
498 expected to be higher for a shorter averaging interval such as 6 hours. Therefore, completely
499 correcting the difference in mean *NEE* slightly overcorrects systematic differences in *NEE*. In
500 general results were not very sensitive to different moving average sizes of the sfd-correction
501 term and data coverage percentages defined for this interval (Tab.A3).

502 It is expected that systematic differences in measured *NEE* caused by spatially variable land
503 surface properties are stronger during the night than during the day since they affect
504 respiration more directly than photosynthesis (see e.g. Oren et al., 2006). Moreover, during
505 night-time and/or winter (positive *NEE*), some conditions associated with lower EC data
506 quality such as low turbulence, strong stability, and liquid water in the gas analyzer path
507 prevail more often than in summer and/or daytime (negative *NEE*). The less severe cases of
508 such conditions are not always completely eliminated by the quality control. In time series of
509 eddy-covariance fluxes this typically shows up as implausible fluctuations of the flux during
510 calm nights. This is reflected by plots of *NEE* flux magnitude versus uncertainty (Fig.2-3;

511 Fig.5-6) showing higher uncertainties for positive compared to negative *NEE* data which
512 agrees with previous findings (e.g. Richardson et al., 2006).

513 At very large EC tower distances (20.5 km, 34 km) footprints were not overlapping and the
514 environmental conditions were considerably different; in particular for the EC tower setup
515 Rollesbroich/Merzenhausen with different land use (grassland/crop) and climate conditions.
516 For those distances, the relative difference $\Delta \sigma_{\text{cov}}$ between σ_{cov} and $\sigma(\delta)$ (classical two-tower
517 approach) was much larger than $\Delta \sigma_{\text{cov}}$ between σ_{cov} and $\sigma(\delta)_{\text{corr,f}}$ (extended two-tower
518 approach). $\Delta \sigma_{\text{cov}}$ was reduced by 85.7% for the 20.5km distance and 79.3% for the 34km if
519 both sfd-correction and weather filter were used. However, after applying the sfd-correction
520 and the weather-filtering, the mean uncertainty estimate was still higher than the raw-data
521 based reference value (Tab.2), suggesting that for these large EC tower distances the sfd-
522 correction and the weather-filter do not fully capture systematic flux differences and
523 uncertainty is still overestimated by the extended two-tower approach. This can have
524 different reasons. We assume the major reason is that the weather-filter is supposed to
525 capture all measured flux differences that can be attributed to different weather conditions at
526 both EC towers which cannot be captured with the sfd-correction. Applying stricter
527 thresholds could increase the efficiency of the weather filter but in our case the reduced
528 dataset was too small to allow further analysis. In general, the weather-filter did not improve
529 the uncertainty estimates as much as the sfd-correction. However, this does not imply that
530 differences in weather conditions are negligible when applying the extended two-tower
531 approach for larger EC tower distances. In fact the systematic part of measured EC flux
532 differences between both towers caused by (steady, systematic) among-site differences in
533 weather conditions were already partly captured with the sfd-correction. In contrast, such

534 systematic differences were difficult to capture with the weather-filter because much lower
535 thresholds would have been required.

536 The absolute corrected and weather-filtered uncertainty value $\sigma(\delta)_{\text{corr,f}}$ [$\mu\text{mol m}^{-2} \text{s}^{-1}$] was
537 slightly lower for the 34 km EC tower distance than for the 20.5 km EC tower distance
538 (Tab.2). The raw-data based reference σ_{cov} [$\mu\text{mol m}^{-2} \text{s}^{-1}$] however was also smaller for the 34
539 km dataset than for the 20.5 km dataset which can be related to the different lengths and
540 timing (i.e., different seasons) of the measurement periods for each of the five EC tower
541 distances: The roving station was moved from one distance to another within the entire
542 measurement period of ~ 27 months. During this entire time period of data collection, the
543 length and timing of the single measurement periods varied for the five EC tower separation
544 distances (Tab.1). This is not optimal because the random error is directly related to the flux
545 magnitude and the flux magnitude itself is directly related to the timing of the measurements.
546 Because in spring and summer flux magnitudes are higher, the random error is generally
547 higher as well (Richardson et al., 2006). To reduce this effect, we captured spring/summer as
548 well as autumn/winter months in each measurement period. However, the timing of the
549 measurements and the amount of data available were not the same for the five EC datasets. In
550 particular the permanent EC tower in Merzenhausen was measuring considerably longer (> 2
551 years) than the roving station did for the other four EC tower distances. Therefore,
552 differences of the mean uncertainty estimates for the five measurement periods were partly
553 independent of the EC tower distance. This effect gets obvious when looking at the mean
554 uncertainties σ_{cov} estimated with the reference method, which should be independent of the
555 distance but were also found to be different for each dataset of the five EC tower distances.
556 Against this background, statements about how EC tower distances affect the two-tower
557 based uncertainty estimate need to be treated with caution.

558 The *NEE* uncertainty $\sigma(\delta)_{\text{corr},f}$ estimated for the grassland site Rollesbroich agree well with
559 the *NEE* uncertainty values for grassland sites by Richardson et al. (2006), and also the
560 regression coefficients (Fig. 2-3; Fig.5-6, Tab. A1) do not show large differences. This can be
561 expected since Richardson et al. (2006) applied their method for a very well-suited tower pair
562 with low systematic differences, such that the classical approach and our extended approach
563 should approximately converge. However, identical results are unlikely because even for two
564 very similar neighboring sites some systematic differences occur. In addition, the random
565 error is expected to vary between sites (see e.g. Mauder et al., 2013) which is in part related
566 to instrumentation.

567 **5 Conclusions**

568 When estimating the uncertainty of eddy covariance net CO₂ flux (*NEE*) measurements with
569 a two-tower based approach it is important to consider that the basic assumptions of identical
570 environmental conditions (including weather conditions and land surface properties) on the
571 one hand and non-overlapping footprints on the other hand are contradicting and impossible
572 to fulfill. If the two EC towers are located in a distance large enough to ensure non
573 overlapping footprints, different environmental conditions at both EC towers can cause
574 systematic differences of the simultaneously measured fluxes that should not be included in
575 the uncertainty estimate. This study for the grassland site Rollesbroich in Germany showed
576 that the extended two-tower approach which includes a correction for systematic flux
577 differences (sfd-correction) can be used to derive more reliable (less overestimated)
578 uncertainty estimates compared to the classical two-tower approach. An advantage of this
579 extended two-tower approach is its simplicity and the fact that there is no need to quantify the
580 differences in environmental conditions (which is usually not possible due to a lack of data).
581 Comparing the uncertainty estimates for five different EC tower distances showed that the

582 mean uncertainty estimated with our extended two-tower approach for the 95 m and 173 m
583 distances were nearly identical to the random error estimated with the raw-data based
584 reference method. This suggests that these distances were most appropriate for the
585 application of the extended two-tower approach in this study. Accordingly, we consider the
586 regressions in Fig.6 (b,c) to be most reliable. Also for the largest EC tower distances (20.5
587 km, 34 km) the sfd-correction significantly improved the correlations of the flux magnitude
588 and the random error and significantly reduced the difference to the independent, raw data
589 based reference value. We therefore conclude that if no second EC tower is available at a
590 closer distance (but available further away), a rough, probably overestimated *NEE*
591 uncertainty estimate can be acquired with the extended two-tower approach although
592 environmental conditions at the two sites are not identical.

593 A statement about the transferability of our experiment to other sites and EC tower distances
594 requires further experiments. However, we assume transferability is given if both EC towers
595 are located at sites of the same vegetation type (e.g. C3-grasses, C4-crops, deciduous forest,
596 coniferous forest, etc.). Flux differences caused by a different phenology can be very hard to
597 separate from the random error estimate, even though they are expected to be mainly
598 systematic and could therefore be partly captured with the sfd-correction. Moreover, the EC
599 raw data should be processed in the same way (as done here) and the measurement devices
600 should be identical and installed at about the same measurement height. Important is also that
601 the instruments are calibrated thoroughly and consistently. Because this was true for the three
602 EC towers included in this study, we conclude that systematic flux differences that are
603 corrected for with the sfd-correction arise mainly from different environmental conditions
604 whereas calibration errors are assumed to have a very minor effect. Different weather
605 conditions at both EC tower sites are a main drawback for applications of the two-tower

606 approach. While systematic differences of the weather conditions are expected to be captured
607 by the sfd-correction, less systematic weather fluctuations e.g. related to cloud movement, are
608 difficult to be filtered of the two-tower based uncertainty estimate. Applying very strict
609 thresholds can lead to a too small dataset, especially if the measurement periods are short. If
610 EC raw data is available, we recommend to use an uncertainty estimation scheme like the one
611 presented in Mauder et al. (2013). Raw-data based NEE uncertainty estimation methods like
612 the one suggested by Finkelstein and Sims (2001) and implemented by Mauder et al. (2013)
613 have not been extensively applied yet and – to the best of our knowledge – never been
614 compared to the ones derived with the more well-known two-tower approach. The fact that
615 the two uncertainty estimates (extended two-tower approach and raw-data based reference)
616 give very similar results therefore contributes to the confidence in both methods.

617 Appendix A

618 Tab. A1

619 *Summary of the 95% confidence intervals for the linear regression coefficients of the NEE*
620 *magnitudes - standard error relationships determined with Eq.1 for the four two two-tower based*
621 *correction schemes and the five EC tower distances*

Variables:	Two towers:	m	m _{lower}	m _{upper}	b	b _{lower}	b _{upper}
NEE_{negative} / σ(δ)	EC1 / EC2 (8 m)	-0.012	-0.041	0.017	0.691	0.442	0.940
	EC1 / EC2 (95 m)	-0.045	-0.099	0.010	1.163	0.680	1.647
	EC1 / EC2 (173 m)	-0.052	-0.067	-0.036	1.747	1.537	1.957
	EC1 / EC2 (20.5 km)	-0.088	-0.272	0.097	2.544	0.696	4.392
	EC1 / EC3 (34 km)	-0.130	-0.330	0.069	2.849	0.772	4.926
NEE_{negative} / σ(δ)_f	EC1 / EC2 (8 m)	-0.008	-0.043	0.026	0.746	0.497	0.995
	EC1 / EC2 (95 m)	-0.005	-0.036	0.026	1.569	1.286	1.853
	EC1 / EC2 (173 m)	-0.055	-0.088	-0.021	1.416	1.009	1.824
	EC1 / EC2 (20.5 km)	-0.011	-0.087	0.066	2.606	1.929	3.284
	EC1 / EC3 (34 km)	-0.039	-0.190	0.113	3.527	1.737	5.317
NEE_{negative} / σ(δ)_{corr}	EC1 / EC2 (8 m)	-0.036	-0.048	-0.024	0.227	0.125	0.329
	EC1 / EC2 (95 m)	-0.043	-0.072	-0.014	0.699	0.379	1.018
	EC1 / EC2 (173 m)	-0.052	-0.087	-0.017	0.485	-0.059	1.030
	EC1 / EC2 (20.5 km)	-0.085	-0.142	-0.028	1.033	0.312	1.754
	EC1 / EC3 (34 km)	-0.092	-0.129	-0.055	0.963	0.421	1.505
NEE_{negative} / σ(δ)_{corr,f}	EC1 / EC2 (8 m)	-0.040	-0.060	-0.019	0.211	0.053	0.369
	EC1 / EC2 (95 m)	-0.044	-0.074	-0.013	0.574	0.252	0.895
	EC1 / EC2 (173 m)	-0.071	-0.122	-0.021	0.272	-0.440	0.983
	EC1 / EC2 (20.5 km)	-0.106	-0.204	-0.009	0.493	-0.685	1.671

	EC1 / EC3 (34 km)	-0.070	-0.108	-0.031	0.981	0.346	1.616
NEE_{positive} / $\sigma(\delta)$	EC1 / EC2 (8 m)	0.101	0.027	0.174	0.346	-0.024	0.715
	EC1 / EC2 (95 m)	0.161	0.028	0.294	0.734	0.285	1.183
	EC1 / EC2 (173 m)	0.061	-0.284	0.406	1.340	-0.775	3.455
	EC1 / EC2 (20.5 km)	0.118	-0.272	0.507	1.332	-0.500	3.164
	EC1 / EC3 (34 km)	0.235	0.113	0.356	0.731	0.323	1.140
NEE_{positive} / $\sigma(\delta)_f$	EC1 / EC2 (8 m)	0.101	0.020	0.182	0.340	-0.080	0.760
	EC1 / EC2 (95 m)	0.029	-0.299	0.357	1.333	-0.114	2.780
	EC1 / EC2 (173 m)	0.179	-0.122	0.480	0.535	-1.316	2.385
	EC1 / EC2 (20.5 km)	0.145	-0.174	0.464	1.134	-0.365	2.632
	EC1 / EC3 (34 km)	0.320	0.059	0.580	0.763	-0.330	1.857
NEE_{positive} / $\sigma(\delta)_{corr}$	EC1 / EC2 (8 m)	0.083	0.043	0.123	0.089	-0.106	0.284
	EC1 / EC2 (95 m)	0.074	0.054	0.094	0.165	0.094	0.236
	EC1 / EC2 (173 m)	0.172	-0.093	0.436	-0.110	-1.979	1.759
	EC1 / EC2 (20.5 km)	0.245	0.122	0.367	-0.328	-0.938	0.282
	EC1 / EC3 (34 km)	0.162	0.135	0.189	0.080	-0.015	0.175
NEE_{positive} / $\sigma(\delta)_{corr,f}$	EC1 / EC2 (8 m)	0.078	0.037	0.118	0.101	-0.102	0.303
	EC1 / EC2 (95 m)	0.090	0.030	0.150	0.136	-0.142	0.414
	EC1 / EC2 (173 m)	0.163	-0.132	0.459	-0.040	-2.081	2.000
	EC1 / EC2 (20.5 km)	0.159	-0.094	0.413	0.072	-1.205	1.349
	EC1 / EC3 (34 km)	0.205	0.132	0.279	0.029	-0.278	0.337

* m_{lower} ; m_{upper} : lower and upper 95% confidence interval for slope m

* b_{lower} ; b_{upper} : lower and upper 95% confidence interval for intersect b

$\sigma(\delta)$, $\sigma(\delta)_f$: uncertainty estimated with classical two-tower approach without & with weather filter (f)

$\sigma(\delta)_{corr}$, $\sigma(\delta)_{corr,f}$: uncertainty estimated with extended two-tower approach

Tab. A2: R^2 for NEE uncertainty determined with the extended two-tower approach (including sfd-correction and weather-filter) as function of NEE_{corr} magnitude and for 20.5km EC tower distance. Results are given for different moving average time intervals (6 hr, 12 hr, 24hr) and data coverage percentages (25%, 50%, 70%) for the calculation of the sfd-correction factor (Eq.2)

	6h	12h	24h
30%	0.73; 0.84; (937)	0.92; 0.72; (904)	0.84; 0.82; (597)
50%	0.58; 0.85; (710)	0.7; 0.43; (463)	-; -; (32)
70%	0.77; 0.78; (408)	0.66; 0.08; (148)	-; -; (0)

black: for negative NEE; grey: for positive NEE; (): total number of half-hourly NEE left after sfd-correction and weather filter to build bins for NEE uncertainty versus NEE magnitude regressions (Fig.5 for 12h & 50 %)

622

623 Tab. A3: Relative difference [%] of mean uncertainty $\sigma(\delta)_{corr,f}$ estimated with the extended two
624 tower approach and the reference σ_{cov} for EC tower distances > 8m

Diff	$\Delta\sigma_{cov}$ (6h)	$\Delta\sigma_{cov}$ (12h)	$\Delta\sigma_{cov}$ (24h)
30%	-0.8; 39.3	4.8; 55.5	10.9; 59.9
50%	-9.3; 32.5	-1.5; 41.2	-
70%	-10.5; 24.3	-5.2; 10.2	-

625

black: mean $\Delta\sigma_{cov}$ for 95m and 173m distance ; grey: mean $\Delta\sigma_{cov}$ for 20.5 km and 34 km distance

626 **Acknowledgments.** We are grateful to ExpeER (Experimentation in Ecosystem Research)
627 for funding this work. The eddy covariance data were provided by TERENO and the
628 Transregional Collaborative Research Centre 32 (TR32). We also thank Wittaya Kessomkiat
629 for his support. Moreover, we thank Qu Wei for providing the SoilNet data and Henning
630 Schiedung for providing the soil carbon and soil density data for the Rollesbroich site.

631 **References**

- 632 Allard, V., Soussana, J.-F., Falcimagne, R., Berbigier, P., Bonnefond, J.M., Ceschia, E.,
633 D'hour, P., Hénault, C., Laville, P., Martin, C., Pinarès-Patino, C., 2007. The role of
634 grazing management for the net biome productivity and greenhouse gas budget (CO₂,
635 N₂O and CH₄) of semi-natural grassland. *Agriculture, Ecosystems & Environment*
636 121, 47–58. doi:10.1016/j.agee.2006.12.004
- 637 Ammann, C., Flechard, C.R., Leifeld, J., Neftel, A., Fuhrer, J., 2007. The carbon budget of
638 newly established temperate grassland depends on management intensity. *Agriculture,*
639 *Ecosystems & Environment* 121, 5–20. doi:10.1016/j.agee.2006.12.002
- 640 Arbeitsgruppe BK50, 2001. Allgemeine Informationen zur Bodenkarte 1 : 50 000. - 55 S.;
641 Krefeld (Geol. Dienst Nordrh.-Westf.).
- 642 Aubinet, M., Vesala, T., Papale, D., 2011. *Eddy Covariance: A Practical Guide to*
643 *Measurement and Data Analysis.* Springer Verlag.
- 644 Baldocchi, D.D., 2001. Assessing ecosystem carbon balance: problems and prospects of the
645 eddy covariance technique. *Annual Review of Ecology and Systematics* 33, 1–33.
- 646 Baldocchi, D.D., 2003. Assessing the eddy covariance technique for evaluating carbon
647 dioxide exchange rates of ecosystems: past, present and future. *Global Change*
648 *Biology* 9, 479–492.
- 649 Barr, A.G., Morgenstern, K., Black, T.A., McCaughey, J.H., Nesic, Z., 2006. Surface energy
650 balance closure by the eddy-covariance method above three boreal forest stands and
651 implications for the measurement of the CO₂ flux. *Agricultural and Forest*
652 *Meteorology* 140, 322–337. doi:10.1016/j.agrformet.2006.08.007
- 653 Billesbach, D.P., 2011. Estimating uncertainties in individual eddy covariance flux
654 measurements: A comparison of methods and a proposed new method. *Agricultural*
655 *and Forest Meteorology* 151, 394–405. doi:10.1016/j.agrformet.2010.12.001
- 656 Bogaen, H.R., Huisman, J.A., Meier, H., Rosenbaum, U., Weuthen, A., 2009. Hybrid
657 Wireless Underground Sensor Networks: Quantification of Signal Attenuation in Soil.
658 *Vadose Zone Journal* 8, 755–761. doi:10.2136/vzj2008.0138

- 659 Braswell, B.H., Sacks, W.J., Linder, E., Schimel, D.S., 2005. Estimating diurnal to annual
660 ecosystem parameters by synthesis of a carbon flux model with eddy covariance net
661 ecosystem exchange observations. *Global Change Biology* 11, 335–355.
662 doi:10.1111/j.1365-2486.2005.00897.x
- 663 Dragoni, D., Schmid, H.P., Grimmond, C.S.B., Loescher, H.W., 2007. Uncertainty of annual
664 net ecosystem productivity estimated using eddy covariance flux measurements.
665 *Journal of Geophysical Research-Atmospheres* 112, 1–9. doi:10.1029/2006JD008149
- 666 Finkelstein, P.L., Sims, P.F., 2001. Sampling error in eddy correlation flux measurements.
667 *Journal of Geophysical Research: Atmospheres* 106, 3503–3509.
668 doi:10.1029/2000JD900731
- 669 Flanagan, L.B., Johnson, B.G., 2005. Interacting effects of temperature, soil moisture and
670 plant biomass production on ecosystem respiration in a northern temperate grassland.
671 *Agricultural and Forest Meteorology* 130, 237–253.
672 doi:10.1016/j.agrformet.2005.04.002
- 673 Foken, T., Wichura, B., 1996. Tools for quality assessment of surface-based flux
674 measurements. *Agricultural and Forest Meteorology* 78, 83–105.
- 675 Goulden, M.L., Munger, J.W., Fan, S.M., Daube, B.C., Wofsy, S.C., 1996. Measurements of
676 carbon sequestration by long-term eddy covariance: Methods and a critical evaluation
677 of accuracy. *Global Change Biology* 2, 169–182.
- 678 Herbst, M., Prolingheuer, N., Graf, A., Huisman, J.A., Weihermüller, L., Vanderborght, J.,
679 2009. Characterization and Understanding of Bare Soil Respiration Spatial Variability
680 at Plot Scale. *Vadose Zone Journal* 8, 762. doi:10.2136/vzj2008.0068
- 681 Hill, T.C., Ryan, E., Williams, M., 2012. The use of CO₂ flux time series for parameter and
682 carbon stock estimation in carbon cycle research. *Global Change Biology* 18, 179–
683 193. doi:10.1111/j.1365-2486.2011.02511.x
- 684 Hollinger, D.Y., Aber, J., Dail, B., Davidson, E.A., Goltz, S.M., Hughes, H., Leclerc, M.Y.,
685 Lee, J.T., Richardson, A.D., Rodrigues, C., Scott, N. a., Achuatavarier, D., Walsh, J.,
686 2004. Spatial and temporal variability in forest–atmosphere CO₂ exchange. *Global*
687 *Change Biology* 10, 1689–1706. doi:10.1111/j.1365-2486.2004.00847.x
- 688 Hollinger, D.Y., Richardson, A.D., 2005. Uncertainty in eddy covariance measurements and
689 its application to physiological models. *Tree Physiology* 25, 873–885.
- 690 Kessomkiat, W., Hendricks-Franssen, H.-J., Graf, A., Vereecken, H., 2013. Estimating
691 random errors of eddy covariance data: An extended two-tower approach.
692 *Agricultural and Forest Meteorology* 171, 203–219.
- 693 Kormann, R., Meixner, F.X., 2001. An Analytical Footprint Model For Non-Neutral
694 Stratification. *Boundary-Layer Meteorology* 99, 207–224.
695 doi:10.1023/A:1018991015119

- 696 Korres, W., Koyama, C.N., Fiener, P., Schneider, K., 2010. Analysis of surface soil moisture
697 patterns in agricultural landscapes using Empirical Orthogonal Functions. *Hydrol.*
698 *Earth Syst. Sci.* 14, 751–764. doi:10.5194/hess-14-751-2010
- 699 Kuppel, S., Peylin, P., Chevallier, F., Bacour, C., Maignan, F., Richardson, A.D., 2012.
700 Constraining a global ecosystem model with multi-site eddy-covariance data.
701 *Biogeosciences Discuss.* 9, 3317–3380. doi:10.5194/bgd-9-3317-2012
- 702 Liu, H., Randerson, J., Lindfors, J., Massman, W., Foken, T., 2006. Consequences of
703 Incomplete Surface Energy Balance Closure for CO₂ Fluxes from Open-Path
704 CO₂/H₂O Infrared Gas Analysers. *Boundary-Layer Meteorology* 120, 65–85.
705 doi:10.1007/s10546-005-9047-z
- 706 Lloyd, J., Taylor, J.A., 1994. On the Temperature Dependence of Soil Respiration.
707 *Functional Ecology* 8, 315. doi:10.2307/2389824
- 708 Mauder, M., Cuntz, M., Drüe, C., Graf, A., Rebmann, C., Schmid, H.P., Schmidt, M.,
709 Steinbrecher, R., 2013. A strategy for quality and uncertainty assessment of long-term
710 eddy-covariance measurements. *Agricultural and Forest Meteorology* 169, 122–135.
- 711 Mauder, M., Foken, T., 2011. Documentation and instruction manual of the Eddy covariance
712 software package TK3. Univ. Bayreuth, Abt. Mikrometeorologie.
- 713 Moore, C.J., 1986. Frequency response corrections for eddy correlation systems. *Boundary-*
714 *Layer Meteorology* 37, 17–35. doi:10.1007/BF00122754
- 715 Orchard, V.A., Cook, F.J., 1983. Relationship between soil respiration and soil moisture. *Soil*
716 *Biology and Biochemistry* 15, 447–453. doi:10.1016/0038-0717(83)90010-X
- 717 Oren, R., Hsieh, C.-I., Stoy, P., Albertson, J., McCarthy, H.R., Harrell, P., Katul, G.G., 2006.
718 Estimating the uncertainty in annual net ecosystem carbon exchange: spatial variation
719 in turbulent fluxes and sampling errors in eddy-covariance measurements. *Global*
720 *Change Biology* 12, 883–896. doi:10.1111/j.1365-2486.2006.01131.x
- 721 Qu, W., Bogaen, H.R., Huisman, J.A., Martinez, G., Pachepsky, Y.A., Vereecken, H., 2014.
722 Effects of soil hydraulic properties on the spatial variability of soil water content:
723 evidence from sensor network data and inverse modeling. *Vadose Zone Journal* 13.
- 724 Qu, W., Bogaen, H.R., Huisman, J.A., Vereecken, H., 2013. Calibration of a Novel Low-Cost
725 Soil Water Content Sensor Based on a Ring Oscillator. *Vadose Zone Journal* 12, 1–
726 10. doi:10.2136/vzj2012.0139
- 727 Richardson, A.D., Aubinet, M., Barr, A.G., Hollinger, D.Y., Ibrom, A., Lasslop, G.,
728 Reichstein, M., 2012. Uncertainty Quantification. *Eddy Covariance. A Practical*
729 *Guide to Measurement and Data Analysis* 173–209.
- 730 Richardson, A.D., Hollinger, D.Y., Burba, G.G., Davis, K.J., Flanagan, L.B., Katul, G.G.,
731 William Munger, J., Ricciuto, D.M., Stoy, P.C., Suyker, A.E., Verma, S.B., Wofsy,
732 S.C., 2006. A multi-site analysis of random error in tower-based measurements of
733 carbon and energy fluxes. *Agricultural and Forest Meteorology* 136, 1–18.
734 doi:10.1016/j.agrformet.2006.01.007

- 735 Richardson, A.D., Mahecha, M.D., Falge, E., Kattge, J., Moffat, A.M., Papale, D.,
 736 Reichstein, M., Stauch, V.J., Braswell, B.H., Churkina, G., Kruijt, B., Hollinger,
 737 D.Y., 2008. Statistical properties of random CO₂ flux measurement uncertainty
 738 inferred from model residuals. *Agricultural and Forest Meteorology* 148, 38–50.
 739 doi:10.1016/j.agrformet.2007.09.001
- 740 Tsubo, M., Walker, S., 2005. Relationships between photosynthetically active radiation and
 741 clearness index at Bloemfontein, South Africa. *Theoretical and applied climatology*
 742 80, 17–25.
- 743 Webb, E.K., Pearman, G.I., Leuning, R., 1980. Correction of flux measurements for density
 744 effects due to heat and water vapour transfer. *Quarterly Journal of the Royal*
 745 *Meteorological Society* 106, 85–100.
- 746 Wilson, K., Goldstein, A., Falge, E., Aubinet, M., Baldocchi, D., Berbigier, P., Bernhofer, C.,
 747 Ceulemans, R., Dolman, H., Field, C., Grelle, A., Ibrom, A., Law, B., Kowalski, A.,
 748 Meyers, T., Moncrieff, J., Monson, R., Oechel, W., Tenhunen, J., Valentini, R.,
 749 Verma, S., 2002. Energy balance closure at FLUXNET sites. *Agricultural and Forest*
 750 *Meteorology* 113, 223–243. doi:10.1016/S0168-1923(02)00109-0
- 751 Xu, L., Baldocchi, D.D., Tang, J., 2004. How soil moisture, rain pulses, and growth alter the
 752 response of ecosystem respiration to temperature. *Global Biogeochem. Cycles* 18,
 753 GB4002. doi:10.1029/2004GB002281
- 754 Zacharias, S., Boga, H., Samaniego, L., Mauder, M., Fuß, R., Pütz, T., Frenzel, M.,
 755 Schwank, M., Baessler, C., Butterbach-Bahl, K., Bens, O., Borg, E., Brauer, A.,
 756 Dietrich, P., Hajnsek, I., Helle, G., Kiese, R., Kunstmann, H., Klotz, S., Munch, J.C.,
 757 Papen, H., Priesack, E., Schmid, H.P., Steinbrecher, R., Rosenbaum, U., Teutsch, G.,
 758 Vereecken, H., 2011. A Network of Terrestrial Environmental Observatories in
 759 Germany. *Vadose Zone Journal* 10, 955–973. doi:10.2136/vzj2010.0139

760

761 **Table Captions**

762 Tab. 1. Measurement periods and locations of the permanent EC towers in Rollesbroich
 763 (EC1) and Merzenhausen (EC3) and the roving station (EC2)

764 Tab. 2. Mean NEE uncertainty [$\mu\text{mol m}^{-2} \text{s}^{-1}$] for five EC tower distances estimated with the
 765 classical two-tower approach, with and without including a weather-filter ($\sigma(\delta)$, $\sigma(\delta)_f$
 766). and with the extended two-tower approach (sfd-correction), also with and without
 767 including a weather-filter ($\sigma(\delta)_{\text{corr}}$, $\sigma(\delta)_{\text{corr},f}$). The table also provides the random error
 768 σ_{cov} [$\mu\text{mol m}^{-2} \text{s}^{-1}$] estimated with the raw-data based reference method (Mauder et al.
 769 2013).

770 **Figure Captions**

771 Fig. 1. Eddy covariance (EC) tower locations in the Rur-Catchment (center) including the
 772 Rollesbroich test site (left), with the target areas defined for the footprint analysis

773 Fig. 2. NEE uncertainty $\sigma(\delta)$ determined with the classical two-tower approach as function of
 774 the NEE flux magnitude for the EC tower distances 8m (a), 95m (b) , 173m (c),
 775 20.5km (d) and 34km (e). (Dashed line: linear correlation not significant ($p>0.1$))

776 Fig. 3. NEE uncertainty $\sigma(\delta)$ determined with the classical two-tower approach as function of
 777 the NEE flux magnitude including the application of the weather-filter for the EC
 778 tower distances 8m (a), 95m (b) , 173m (c), 20.5km (d) and 34km (e). (Dashed line:
 779 linear correlation not significant ($p>0.1$))

780 Fig. 4. Scatter of the NEE measured at EC1 (NEE_{EC1}) and NEE measured at a second tower
 781 EC2/EC3 (NEE_{EC2}) for the uncorrected NEE (left) and the sfd-corrected NEE_{corr}
 782 (right) for the EC tower distances 8m (a), 95m (b) , 173m (c), 20.5km (d) and 34km
 783 (e)

784 Fig. 5. NEE uncertainty $\sigma(\delta)_{corr}$ determined with the extended two-tower approach as
 785 function of sfd-corrected NEE_{corr} magnitude (Eq.2) for the EC tower distances 8m (a),
 786 95m (b) , 173m (c), 20.5km (d) and 34km (e) (Dashed line: linear correlation not
 787 significant ($p>0.1$))

788 Fig. 6. NEE uncertainty $\sigma(\delta)_{corr}$ determined with the extended two-tower approach as function
 789 of sfd-corrected NEE_{corr} magnitude (Eq.2) including application of the weather-filter
 790 for the EC tower distances 8m (a), 95m (b) , 173m (c), 20.5km (d) and 34km (e)
 791 (Dashed line: linear correlation not significant ($p>0.1$))

792

793 **Tab. 1. Measurement periods and locations of the permanent EC towers in Rollesbroich (EC1) and**
 794 **Merzenhausen (EC3) and the roving station (EC2)**

	Coordinates	Sitename	Distance to EC1	Measurement period	alt. (m)
EC1	50.6219142 N / 6.3041256 E	Rollesbroich	–	13.05.2011 – 15.07.2013	514.7
EC2	50.6219012 N / 6.3040107 E 50.6219012 N / 6.3040107 E	Rollesbroich	8m	29.07.2011 – 06.10.2011 05.03.2013 – 15.05.2013	514.8
	50.6217990 N / 6.3027962 E 50.6210472 N / 6.3042120 E	Rollesbroich	95m	07.10.2011 – 15.05.2012 01.07.2013 – 15.07.2013	516.3 517.3
	50.6217290 N / 6.3016925 E	Rollesbroich	173m	24.05.2012 – 14.08.2012	517.1
	50.5027500 N / 6.5254170 E	Kall-Sistig	20.5 km	14.08.2012 – 01.11.2012 15.05.2013 – 01.07.2013	498.0
	EC3	50.9297879 N / 6.2969924 E	Merzenhausen	34 km	10.05.2011– 16.07.2013

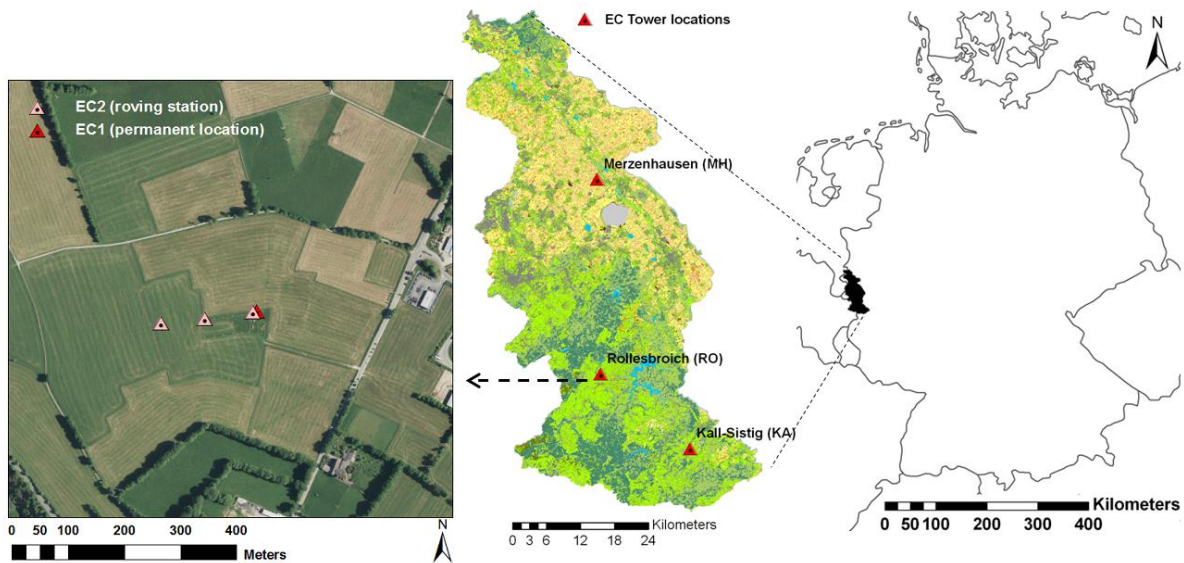
795

796

797 **Tab. 2. Mean NEE uncertainty [$\mu\text{mol m}^{-2} \text{s}^{-1}$] for five EC tower distances estimated with the**
 798 **classical two-tower approach, with and without including a weather-filter ($\sigma(\delta)$, $\sigma(\delta)_f$), and with**
 799 **the extended two-tower approach (sfd-correction), also with and without including a weather-filter**
 800 **($\sigma(\delta)_{\text{corr}}$, $\sigma(\delta)_{\text{corr},f}$). The table also provides the random error σ_{cov} [$\mu\text{mol m}^{-2} \text{s}^{-1}$] estimated with the**
 801 **raw-data based reference method (Mauder et al. 2013).**
 802

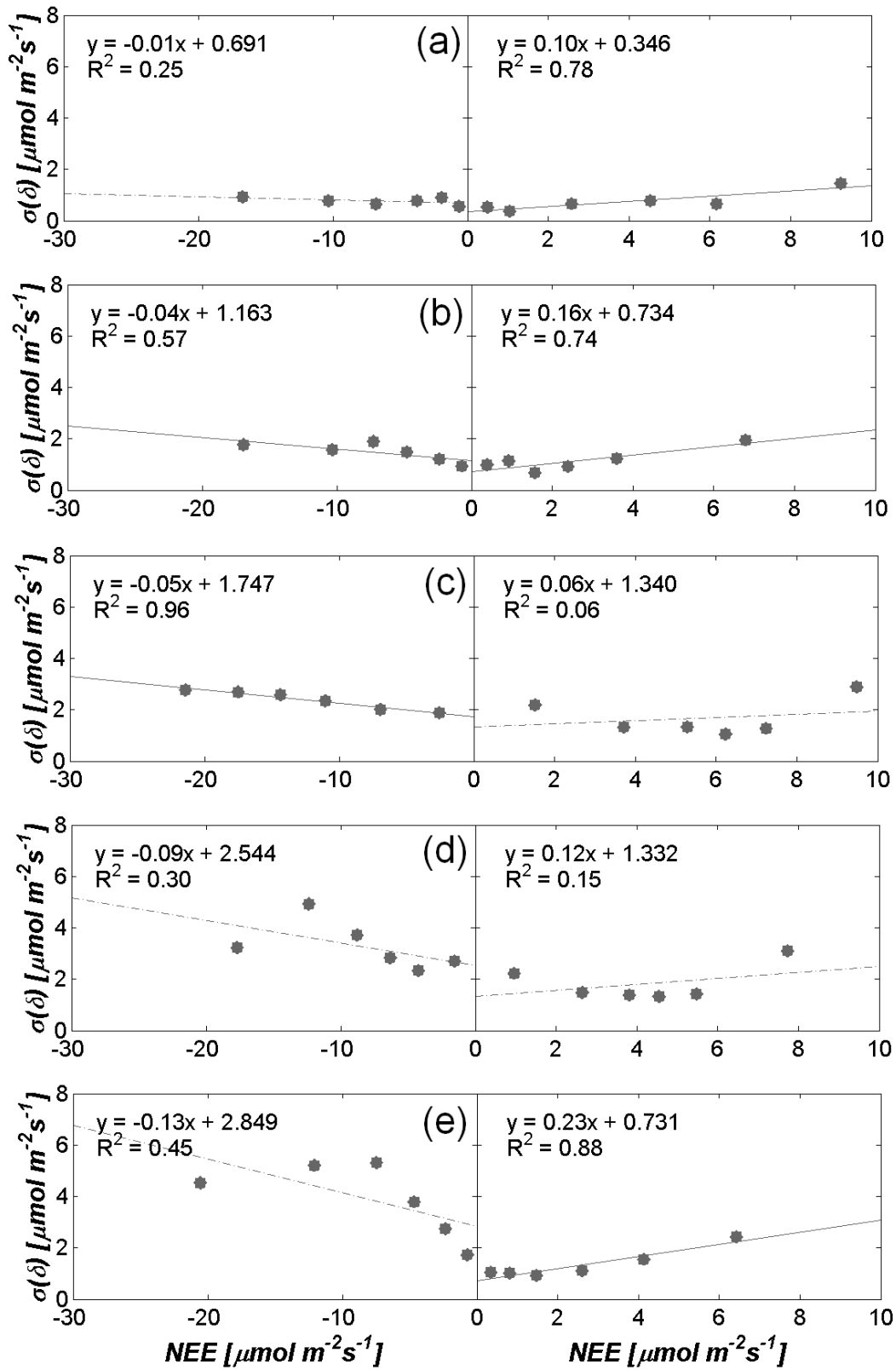
EC tower distance	N	$\sigma(\delta)$ ($\Delta\sigma_{\text{cov}}$)	$\sigma(\delta)_f$ ($\Delta\sigma_{\text{cov}}$)	$\sigma(\delta)_{\text{corr}}$ ($\Delta\sigma_{\text{cov}}$)	$\sigma(\delta)_{\text{corr},f}$ ($\Delta\sigma_{\text{cov}}$)	σ_{cov}
8m	3167	0.76 (18.8)	0.77 (20.5)	0.44 (-30.6)	0.44 (-30.8)	0.64
95m	3620	1.30 (116.7)	1.50 (149.4)	0.65 (8.2)	0.60 (0.2)	0.60
173m	2410	2.04 (98.5)	1.82 (77.0)	1.03 (-0.3)	1.00 (-2.5)	1.03
20.5 km	2574	2.72 (200.6)	2.35 (159.7)	1.52(67.8)	1.16 (28.7)	0.91
34 km	15571	2.73 (274.7)	2.86 (292.4)	1.18 (61.5)	1.14 (56.8)	0.73
mean		1.91	1.86	0.98	0.93	0.78

803 ($\Delta\sigma_{\text{cov}}$): relative differences [%] between two-tower based uncertainty estimates and the references value σ_{cov}
 804 (Eq.4)
 805
 806



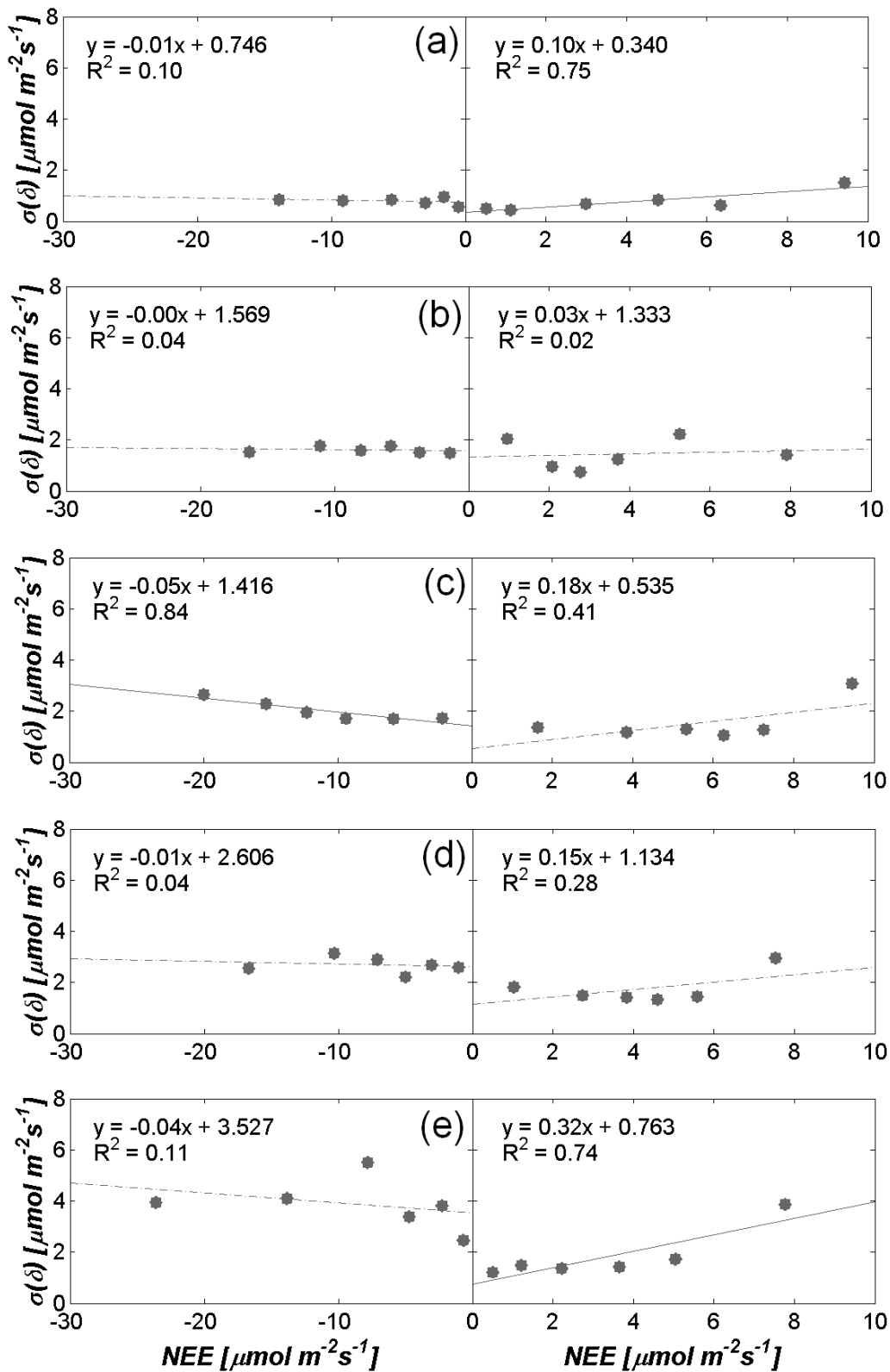
807

808 **Fig. 1. Eddy covariance (EC) tower locations in the Rur-Catchment (center) including the**
 809 **Rollesbroich test site (left)**
 810



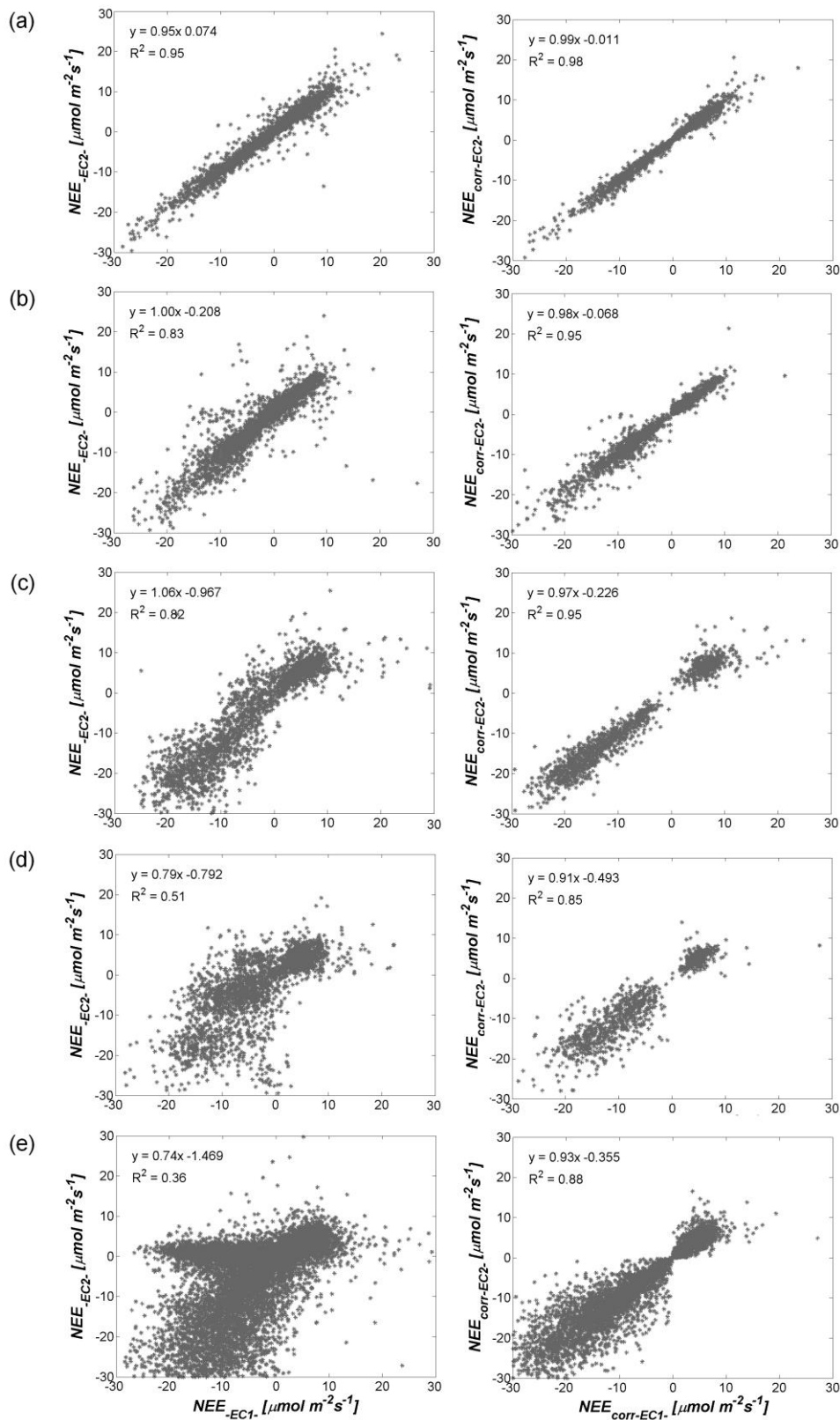
811

812 *Fig. 2. NEE uncertainty $\sigma(\delta)$ determined with the classical two-tower approach as function of the*
 813 *NEE flux magnitude for the EC tower distances 8m (a), 95m (b), 173m (c), 20.5km (d) and 34km*
 814 *(e). (Dashed line: regression slope not significantly different from zero ($p > 0.1$))*



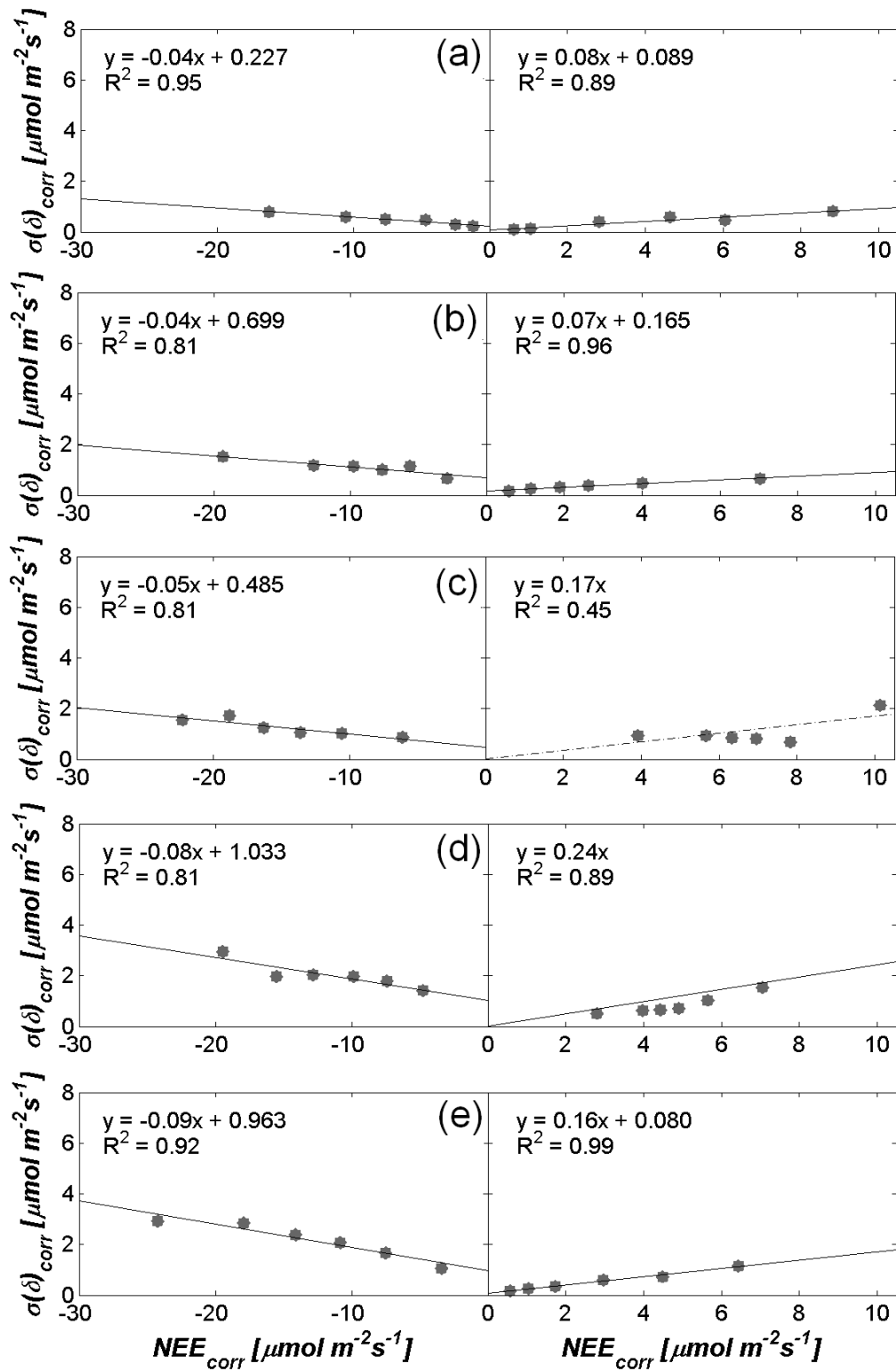
815

816 *Fig. 3. NEE uncertainty $\sigma(\delta)$ determined with the classical two-tower approach as function of the*
 817 *NEE flux magnitude including the application of the weather-filter for the EC tower distances 8m*
 818 *(a), 95m (b), 173m (c), 20.5km (d) and 34km (e). (Dashed line: regression slope not significantly*
 819 *different from zero ($p > 0.1$))*



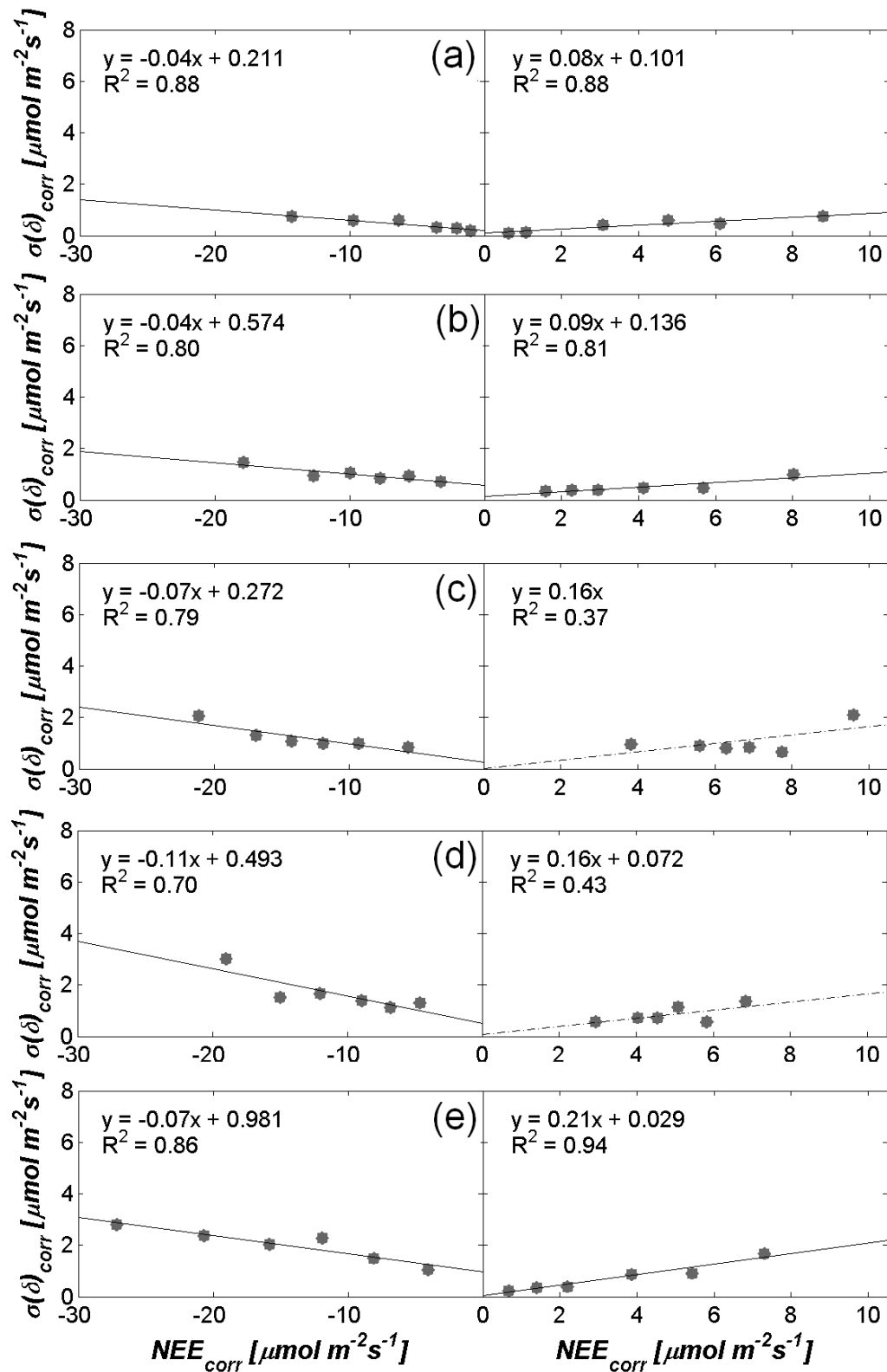
820

821 *Fig.4. Scatter of the NEE measured at EC1 (NEE_{-EC1}) and NEE measured at a second tower*
 822 *EC2/EC3 (NEE_{-EC2}) for the uncorrected NEE (left) and the sfd-corrected NEE_{corr} (right) for the*
 823 *EC tower distances 8m (a), 95m (b) , 173m (c), 20.5km (d) and 34 km*



824

825 *Fig.5. NEE uncertainty $\sigma(\delta)_{corr}$ determined with the extended two-tower approach as function of*
 826 *sfd-corrected NEE_{corr} magnitude (Eq.2) for the EC tower distances 8m (a), 95m (b), 173m (c),*
 827 *20.5km (d) and 34km (e) (Dashed line: regression slope not significantly different from zero*
 828 *($p > 0.1$))*



829

830 *Fig.6. NEE uncertainty $\sigma(\delta)_{corr}$ determined with the extended two-tower approach as function of*
 831 *sfd-corrected NEE_{corr} magnitude (Eq.2) including application of the weather-filter for the EC tower*
 832 *distances 8m (a), 95m (b) , 173m (c), 20.5km (d) and 34km (e) (Dashed line: regression slope not*
 833 *significantly different from zero ($p>0.1$))*